Cognitive Neurodynamics (2020) 14:795–814
https://doi.org/10.1007/s11571-020-09628-z

RESEARCH ARTICLE

Fast fronto-parietal cortical dynamics of conflict detection and context updating in a flanker task

Christopher R. Brydges[1,2] · Francisco Barceló[3] · An T. Nguyen[1,4] · Allison M. Fox[1,4]

Received: 22 November 2019 / Revised: 4 August 2020 / Accepted: 16 August 2020 / Published online: 24 August 2020

Abstract

Recent research has found that the traditional target P3 consists of a family of P3-like positivities that can be functionally and topographically dissociated from one another. The current study examined target N2 and P3-like subcomponents indexing conflict detection and context updating at low- and high-order levels in the neural hierarchy during cognitive control. Electroencephalographic signals were recorded from 45 young adults while they completed a hybrid go/nogo flanker task, and Residue Iteration Decomposition (RIDE) was applied to functionally dissociate these peaks. Analyses showed a stimulus-locked frontal N2 revealing early detection and fast perceptual categorization of nogo, congruent and incongruent trials, resulting in frontal P3-like activity elicited by nogo trials in the latency-variable RIDE cluster, and by incongruent trials in the response-locked cluster. The congruent trials did not elicit frontal P3-like activity. These findings suggest that behavioral incongruency effects are related to intermediate and later stages of motor response re-programming.

Keywords Response inhibition · Context updating · Conflict detection · Cognitive control · Information theory · Residue iteration decomposition

Introduction

Cognitive control refers to a group of processes associated with performance of specific tasks through appropriate adjustments in executive attention and response selection, whilst minimizing interference from conflicting information (Botvinick et al. 2001, 2004), and is associated with neural activation across a widely distributed fronto-parietal cortical network for cognitive control (Niendam et al. 2012). Event-related potential (ERP) studies have consistently reported a series of peaks putatively contributed by this fronto-parietal network and associated with two temporarily contiguous higher-order cognitive processes: conflict detection and context updating. These two cognitive operations have been most notably associated with the frontal N2 (circa 200–350 ms post-stimulus onset) and the fronto-parietal P3 (circa 300–600 ms post-stimulus onset) ERP components (Gratton et al. 2018; Nguyen et al. 2016; van Veen and Carter 2002). Recent ERP research in task switching, however, has suggested that the traditional division of the P3 complex into a frontal 'novelty' P3a (Courchesne et al. 1975; Friedman et al. 2001; Ranganath and Rainer 2003; Simons et al. 2001; Spencer et al. 1999) and a centro-parietal 'context updating' P3b component (Donchin and Coles 1988; Polich 2007) may be overly simplistic. In turn, new evidence suggests that there may be multiple overlapping and functionally distinct P3-like positivities putatively rising from activation across the fronto-parietal network (Bledowski et al. 2004), each with subtly distinct scalp topographies that are involved in handling rapidly changing cognitive demands (Barceló and Cooper 2018a; Brydges and Barceló 2018; Enriquez-

Electronic supplementary material The online version of this article (https://doi.org/10.1007/s11571-020-09628-z) contains supplementary material, which is available to authorized users.

✉ Christopher R. Brydges
christopherbrydges@gmail.com

[1] School of Psychological Science (M304), University of Western Australia, 35 Stirling Highway, Perth, WA 6009, Australia

[2] Department of Human Development and Family Studies, Colorado State University, Fort Collins, USA

[3] Laboratory of Neuropsychology, University of the Balearic Islands, Majorca, Spain

[4] Neurocognitive Development Unit, School of Psychological Science, University of Western Australia, Perth, Australia

Geppert and Barceló 2018). The aim of the current study was to functionally disentangle these fronto-parietal P3-like positivities, together with the temporally earlier frontal N2, and establish their roles in context updating and conflict detection, respectively.

N2 ERP waveform

The frontal N2 has been described as a fronto-central negativity that is commonly examined in conflict detection and response inhibition tasks such as the go/nogo (a reaction time task that requires participants to respond quickly to target 'go' stimuli and withhold any response to distractor 'nogo' stimuli), and the Eriksen flanker tasks (where a central target stimulus is presented whilst surrounded by potentially distracting flanking stimuli; Nieuwenhuis et al. 2004; Yeung and Nieuwenhuis 2009; Zhou et al. 2019). Frontal N2 amplitude is typically enhanced on infrequently presented nogo and incongruent flanker trials (where the flanking stimuli afford a different response than the central target stimulus) compared to standard go and congruent flanker trials (where the flanking stimuli afford the same response as the central target stimulus), and it is thought to reflect detection of conflict prompting for suppression of pre-potent responses and competing but inappropriate responses (Folstein and Van Petten 2008). Although few studies have directly examined conflict detection during nogo and competing incongruent responses in flanker tasks, recent comparisons using a hybrid nogo/flanker task reported significantly delayed and more posterior N2 effects on incongruent flanker trials compared to nogo trials, suggesting differential engagement of conflict detection during these two cognitive control sub-processes (Brydges et al. 2012, 2013). Additionally, previous fMRI and ERP source localization studies have implicated the anterior cingulate cortex in conflict detection and elicitation of the frontal N2 peak (e.g., Bekker et al. 2005; Botvinick et al. 2004; Carter and van Veen 2007; Fan 2014; van Veen and Carter 2002).

P3 ERP waveform

Traditionally, the P3 waveform has been viewed as a dichotomous component, split into a frontal P3a that is associated with processing of surprising stimuli (Courchesne et al. 1975; Friedman et al. 2001; Ranganath and Rainer 2003; Simons et al. 2001; Spencer et al. 1999), and a parietal P3b component that is thought to index 'context updating' operations (Donchin and Coles 1988; Polich 2007). That is, when the subject updates their model of (or belief about) the environment following a motivationally significant event, then the amplitude of the P3b peak is enhanced (Donchin 1981; Donchin and Coles 1988; Farwell 2012; Friston et al. 2017; Meijer et al. 2013). Alternatively, Verleger (1997) reviewed the use of the P3 waveform in mental chronometry and found that its latency is partly, but not completely, associated with both stimulus encoding and behavioral response time, suggesting that this waveform is strictly locked neither to stimulus nor response onset. Additionally, Verleger (1997) found that response selection in complex choice tasks can result in a second, later P3-like waveform (see also Falkenstein et al. 1994), providing evidence of a multiplicity of functionally distinct fronto-parietal P3-like positivities associated with cognitive control.

Recent task switching ERP research by Barceló and colleagues has also suggested the presence of multiple P3-like positivities overlying fronto-parietal scalp regions, indicating that the P3 component may consist of a number of fronto-parietal positive peaks (Barceló and Cooper 2018a; Brydges and Barceló 2018), expanding early research on subdivisions of the P3 (e.g., Courchesne et al. 1975; Snyder and Hillyard 1976; Squires et al. 1975). Barceló and Cooper (2018a) tested 31 young adults on a two-choice cued task-switching paradigm (a task that required participants to shift task rules and/or stimulus–response mappings), a go/nogo task, and an oddball task (a task that required participants to respond to infrequent target stimuli and not respond to infrequent distractor stimuli), each using identical stimuli but requiring different cognitive and motor demands. They found that a target-locked P3 peak was evoked in all tasks and conditions, providing evidence for a domain general P3 component. Additionally, a large late positive complex (LPC) was also observed when a visual target (requiring a motor response) immediately followed a transition cue (see Dien et al. 2004; Ruchkin and Sutton 1983; and Rushby et al. 2005, for seminal work on the role of the LPC in cognitive control and mental chronometry). Importantly, this LPC component was modulated by cognitive demands formalized as the amount of contextual information conveyed by the stimuli for subsequent response selection (cf., Miller 1956). That is, although the LPC was largest on first target trials immediately following a switch cue (i.e., a visual indication to shift task rule), it was also elicited, albeit at a reduced amplitude, by target trials immediately following a repeat cue (a visual indication to keep using the current task rule), and even after first nogo trials in the go/nogo task. In turn, this LPC was absent several trials after the onset of switch/repeat cues, nogo events, and throughout the oddball task. These graded modulations in target P3-like activity tracked dynamic trial-by-trial changes in contextual information. Barceló and Cooper (2018a) analyzed the current source densities of target P3 (300–350 ms) and target LPC (400–1100 ms) at electrode sites overlying fronto-parietal regions, and reported fast

changing and subtle but significant differences in scalp topography, implying different configurations of fronto-parietal generators for different P3-like sub-components in first target trials. The fronto-parietal distribution of the P3/LPC complex has been linked to widespread activation across a fronto-parietal network (Bledowski et al. 2004), including the lateral prefrontal cortex, temporo-parietal junction, and pre-supplementary motor area (Niendam et al. 2012), consistent with a fronto-parietal multiple demand system for cognitive control (Duncan 2010), and with groundbreaking early work on subdivisions of the P3 complex (e.g., Courchesne et al. 1975; Dien et al. 2004; Donchin 1981; Johnson and Donchin 1985; Snyder and Hillyard 1976; Spencer et al. 1999; Squires et al. 1975).

One limitation of traditional ERP analyses to examine neurophysiological processes is that they are typically locked to a particular task event—generally either a sensory stimulus or a motor response (Luck 2014)—when both stimulus-locked and response-locked activity are elicited within the same time epoch, and hence, they potentially temporally overlap each other. As a consequence, an ERP that is locked to trial-variable reaction times (RTs) will not show a clear peak and will be smeared within the stimulus-locked ERP waveform, and vice versa. In an attempt to counter this, Ouyang and colleagues (Ouyang et al. 2011, 2013, 2015, 2016, 2017) developed a novel method for separating ERP components based on the variability of single trial latencies, namely residue iteration decomposition (RIDE; see also Güntekin and Başar 2010, for an alternate method to explore the multiplicity of P3-like sub-component structure). This technique defines clusters of components that are either stimulus-locked (S cluster), response-locked (R cluster), or neither (i.e., affected partially, but not completely, by RT—referred to henceforth as the central C cluster). The RIDE technique is implemented by iteratively calculating correlations between estimates of stimulus-locked and response-locked components and EEG waveforms across single trials (Ouyang et al. 2011).

Brydges and Barceló (2018) applied RIDE analyses to EEG data on the same two-choice cued switching task, and showed a variety of functionally distinct albeit topographically similar P3-like positivities across fronto-parietal regions for each of the stimulus-locked, response-locked, and latency-variable (central) clusters, each with subtly distinct amplitude and topographical modulations occurring as a function of trial-by-trial demands. Specifically, regular P3-like (300–350 ms) peaks were observed in all three clusters and were modulated by task-specific contextual information, implying that the context updating hypothesis of P300 elicitation (Donchin and Coles 1988) may be reconceptualized in terms of trial-by-trial updating of the mental model of the task (aka the "task-set") putatively being held at fronto-parietal networks (Friston et al. 2017; Jepma et al. 2016). A corollary of this new proposal is that context updating can be triggered by adjustments at various levels in the putative hierarchy of cognitive control (Brydges and Barceló 2018), either due to changes in sensory input, changes in motor responses, and/or changes in low- and high-order intermediate sensorimotor processes (Fig. 1a; Miller and Cohen 2001). Additionally, some of these fronto-parietal P3-like positivities showed a more frontal scalp distribution under some specific trial conditions, thus reflecting rapid increases in frontal information processing resources dynamically engaged to meet trial-by-trial changes in cognitive demands (Koechlin and Summerfield 2007). In sum, these results suggest that the target P3 complex consists of several functionally and topographically distinct stimulus-locked, intermediate latency-variable, and response-locked P3-like positivities contributed by a widely distributed fronto-parietal network (Niendam et al. 2012). This newly proposed P3 taxonomy implies multiple functionally and temporally distinct, though partly overlapping context updating operations that can be extracted from the traditional ERP waveform.

Miller and Cohen's (2001) theory of prefrontal function

Miller and Cohen (2001) posited that "cognitive control stems from the active maintenance of patterns of activity in the prefrontal cortex that represent goals and the means to achieve them" (p. 167). Accordingly, one function of the prefrontal cortex is to supervise and coordinate signals to and between other neural regions that are responsible for encoding incoming information (e.g., a stimulus), applying various rules to the information (e.g., response conflict resolution), and the resulting output (e.g., selecting an appropriate response). This coordination aspect is especially important when presented stimuli are ambiguous (i.e., activate more than one input–output pathway), thus causing response conflict. The schematic representation shown in Fig. 1a illustrates these postulated operations, highlighting the low-level sensory processing units indicative of neural representations of the sensory event together with response processing units indicative of the selection of the appropriate response options. Further, according to Miller and Cohen's (2001) schematic, the prefrontal cortex accommodates higher-order 'hidden' or 'latent' variables, whose role is to activate and coordinate low-order neural pathways to ensure the selection of the appropriate response. These are referred to as 'hidden' units because they cannot be directly observed and need to be inferred from the information exchanges between an agent and its environment (i.e., "which means computing the posterior probability of (unknown or hidden) causes,

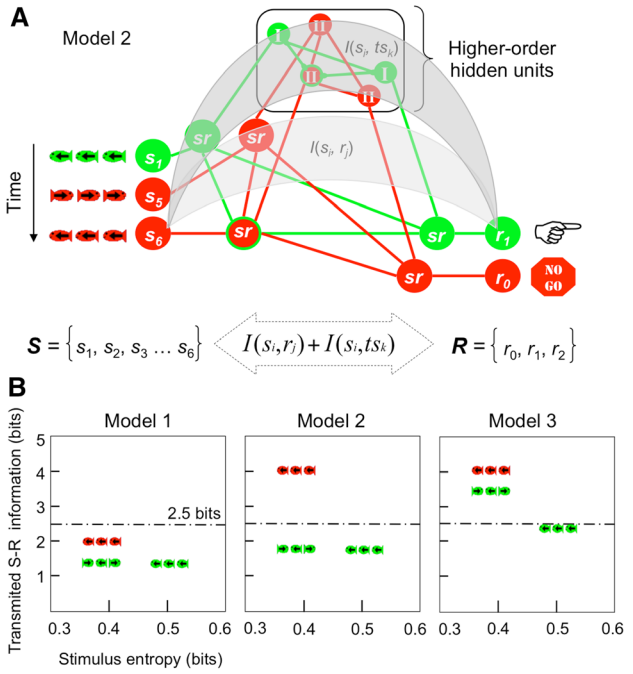

Fig. 1 Formal modelling of cognitive demands in the flanker task. **a** An integrative model of prefrontal executive control (adapted from Miller and Cohen 2001) was adopted to formalize contextual information in the flanker task in terms of all sensory, motor and intermediate low- and high-order sensorimotor representations (or hidden units), as well as their probabilistic interdependencies, inasmuch as an active working memory representation of all those elements was necessary for efficient flanker task performance. For simplicity, only three trial types are illustrated here, namely, a congruent row of green left-facing fish is mapped onto a left-hand response, whereas two rows of red fish are mapped onto a nogo response. Actual stimulus displays consisted of five green or red fish in a row, and the full stimulus set consisted on six stimulus exemplars that could be mapped either to left-hand, right-hand, or nogo responses. Cognitive demands were estimated in terms of sensorimotor information transmission across both low- and high-order levels within the putative hierarchy of cognitive control. **b** A priori estimations of transmitted information, $I(s_i, r_j) + I(s_i, ts_k)$, between stimuli and responses as a function of stimulus entropy, $H(s_i) = -p(s_i) \cdot \log_2 p(s_i)$, of congruent, incongruent and nogo stimuli. The information transmitted from stimuli to responses is derived from the notion of mutual information, $I(S; R)$, between the set of all stimuli, S $\{s_1, s_2, s_3, s_4, s_5, s_6\}$, and their associated responses, R $\{r_0, r_1, r_2\}$ (cf. Attneave 1959; Koechlin and Summerfield 2007; see details in Supplementary material). The dotted line marks the theoretical human capacity for holding information in working memory: 2.5 bits (cf. Miller 1956). Accordingly, the same trial type could convey different amounts of transmitted information depending on the hypothetical number of high-order hidden units assumed to account performance in the flanker task. Model 1: 1 hidden unit, predicts no frontal ERP differences between task conditions; model 2: 2 hidden units, predicts frontal differences between green (congruent and incongruent go conditions) and red (nogo) stimuli; model 3: 3 hidden units, predicts frontal differences between all three task conditions (see the main text for a full explanation). (Color figure online)

given observed outcomes"; Friston et al. 2017 p. 7). These high-order hidden units are assumed to be held at prefrontal cortices and they arbitrate the information flow between sensory stimuli and motor responses (or sensorimotor processes) at lower levels in the neural hierarchy.

Figure 1a provides an illustration of Miller and Cohen's (2001) model. The stimuli from the hybrid flanker go/nogo task used in the current study are on the left, the response options are on the right, and in the middle are hidden units (though in order to keep the model simple, only three of six possible stimulus types are shown, including no incongruent stimuli, and only two out of three possible response options). An example of such hidden units is any simple rule of action for goal-directed behavior (i.e., 'press the left button for all left-looking green fish', or 'do not respond to any red fish'). In Fig. 1a, the role of high-order hidden variables in prefrontal cortex is to activate and coordinate low-level neural pathways so that presentation of a red nogo stimulus results in no response being made. From this view, prefrontal cortex guides the flow of neural activity to update stimulus–response mappings for the current nogo trial (i.e., no response is to be made), through the neural node(s) involved in inhibiting a motor response. From there, these pathways can be strengthened through repeated practice and successful learning. The hierarchical structure of this model of prefrontal function is compatible with the multiple and functionally distinct high- and low-order context updating processes to surprising stimulation posited by the reformulated hypothesis of P3 elicitation (cf., Barceló and Cooper 2018b; Brydges and Barceló 2018).

The current study

The current study aimed to extend previous results by examining target N2 and P3-like sub-components indexing conflict detection and context-updating processes at both low- and high-order levels in the neural hierarchy during cognitive control in a flanker task. In doing so, we adopted a well-known model of prefrontal executive control (Miller and Cohen 2001; Fig. 1a), together with formal information theory estimates of cognitive demands associated with the processing of nogo, congruent, and incongruent flanker trials (Fig. 1b; cf., Cooper et al. 2016; Koechlin and Summerfield 2007; Miller 1956; Zénon et al. 2019). This formal framework helped us characterize the relative contribution from between-condition differences in sensory, motor and intermediate sensorimotor hidden units towards the updating of the ongoing task context, as the participants' uncertainty about any of the changes was assumed to elicit conflict detection (frontal N2) and context updating (fronto-parietal P3) operations (Barceló and Cooper 2018a; Fan 2014; Friston et al. 2017; Parr et al. 2020). The task context was defined as any sensory, motor, or intermediate sensorimotor neural representations (also high-order hidden units; Fig. 1a), as well as their probabilistic interdependencies (cf. Friston et al. 2017),

inasmuch as an active working memory representation of all those elements is necessary for efficient task performance. The task consisted of a hybrid go/nogo flanker task (Brydges et al. 2012, 2013) where a congruent row of green fish was to be categorized using left or right button presses according to the direction of the central fish. In 25% of trials, the direction of the central fish was incongruent to that of surrounding flanker fish. Further, 'nogo' trials (25% of trials) consisted of congruent fish presented in a different color (red). Through explicit task instructions and practice, participants acquired the correct stimulus–response (S–R) mappings to be implemented through low-order sensorimotor S–R links (Fig. 1a). Importantly, the dynamic engagement of prefrontal executive resources on a trial-by-trial basis was hypothesized to depend on the number of high-order hidden units necessary for regulating the dynamic updating of a constant number of low-order sensorimotor units at posterior association cortices, with a larger number of high-order hidden units requiring larger prefrontal resources. The dynamic trial-by-trial changes in cognitive demands associated with the processing of different flanker stimuli could thus be modelled as information transmission through hypothetical high-order hidden units (Fig. 1a, b; cf. Fan 2014; Friston et al. 2017; Parr et al. 2020), with one high-order hidden unit implying no transmission of information through prefrontal cortices (model 1; Fig. 1b), and progressively larger numbers of high-order hidden units involving gradually larger amounts of information transmission through prefrontal regions (Fig. 1b; Table 1; see Supplementary materials). The feasibility of each of these models was then assessed using Bayesian analyses of the electrophysiological evidence provided by RIDE decomposed target N2 and P3-like activity from the S, C and R clusters, and specifically the activity recorded over frontal scalp regions. Consequently, the absence of task differences in any RIDE cluster over frontal regions would support model 1 (i.e., just one high-order hidden unit). In turn, significant differences between all congruent, incongruent, and nogo task conditions over frontal regions in some of the RIDE clusters would lend support to model 3 (see Fig. 1b).

Admittedly, this is a relatively novel approach to examine the context updating hypothesis of P300 elicitation that considers it as a summation of information processes at both low-order (post-rolandic, P3b) and high-order (pre-rolandic, P3a) multimodal association cortices of fronto-parietal networks, with progressively larger information processing demands recruiting progressively more frontal regions (cf., Barceló and Cooper 2018a, b; Brydges and Barceló 2018). However, this hierarchical view of cognitive control is consistent with new active Bayesian inference theories of brain function (e.g., Friston et al. 2017), as well as widely accepted models of prefrontal function (Koechlin and Summerfield 2007; Miller and Cohen 2001). Moreover, this is also in line with recent modeling work suggesting that the anterior P3a and posterior P3b sub-components encode Bayesian belief updating at two distinct levels in the neural hierarchy (Kopp and Lange 2013; Kopp et al. 2016). In order to examine this hypothesis further, information transmission between hidden variables and potential outcomes or responses in our flanker task was modeled (Table 1; Supplementary materials) following a very simple approach similar to that of Koechlin and Summerfield (2007), who were inspired on the pioneering work by Miller (1956) in defining the capacity limits of humans for processing information. Additionally, there is a direct mathematical correspondence between the algorithms used by the hierarchical Bayesian modeling of belief updating (Friston et al. 2017; Parr et al. 2020) and the conditional and joint probabilities used in our information theory metrics for estimating information transmission (Doya and Ishii 2007). In sum, our simple modeling of information transmission (Table 1) predicts larger information processing demands with a larger number of hidden variables involved at high-order levels in the neural hierarchy of control (cf., Friston et al. 2017; Parr et al. 2020).

Under the assumption that the frontal N2 is elicited as a result of conflict detection (Fan 2014; Folstein and van Petten 2008; Nguyen et al. 2016; van Veen and Carter 2002), whereas the target P3 is elicited as a result of context updating operations to surprising stimulation

Table 1 Modeling of transmitted S–R information (in bits) for the three task conditions in Fig. 1, as a function of the number of hypothetical high-order hidden units

Task conditions	Model 1 (1 hidden unit)	Model 2 (2 hidden units)	Model 3 (3 hidden units)
Congruent	1.42	1.84	2.42
Incongruent	1.42	1.84	3.42
NoGo	2.00	4.00	4.00
Low-order $\Sigma\ I(s_i, r_j)$	4.84	4.84	4.84
High-order $\Sigma\ I(s_i, ts_k)$	0.00	2.84	5.00

Models considering different high-order hidden units for left and right stimuli and responses were dismissed as implausible, given evidence of similar target N2 and P3 responses irrespective of the left versus right direction of flanker stimuli. For technical details, see Supplementary materials

(Barceló and Cooper 2018a; Donchin and Coles 1988; Friston et al. 2017; Jepma et al. 2016), the current study aimed to examine how many prefrontal higher-order hidden variables control behavior in this flanker task. Several hypotheses can be derived from the theoretical rationale described above, depending on the number of high-order hidden units involved in producing efficient flanker task behavior. For instance, if only one high-order hidden unit was needed (model 1), then electrophysiological differences between task conditions should not be apparent over frontal regions in any of the RIDE clusters. Alternatively, our model's predictions differ depending on whether two high-order hidden units (i.e., one to categorize the frequent green targets, and one to categorize the infrequent red nogo trials; model 2), or three hidden units were involved (i.e., one for frequent congruent targets, one for infrequent incongruent targets, and one for infrequent nogo trials; model 3, Fig. 1b), with larger task differences in N2 and P3 amplitudes over frontal regions predicted for those task conditions requiring larger prefrontal working memory demands (reflected by the 2.5 bit limit in each model in Fig. 1b; cf. Miller 1956). That is, model 1 predicts no differences in frontal ERP activity between any task conditions, model 2 predicts frontal differences only between green (i.e., congruent and incongruent conditions) and red (nogo) stimuli, and model 3 predicts frontal differences between all three task conditions. These models assume the same amount of transmitted information through low-level sensorimotor pathways for the six S–R links required to perform the task. Hence, any differences among models depend on the number of hidden high-order hidden units in the hierarchy of control (Fig. 1a; Table 1). As such, it was expected that high-order conflict detection (reflected in the frontal N2 peak) would be more likely to also elicit high-order context updating (frontal P3a activity). Additionally, based on Brydges and Barceló's (2018) revised version of the context updating theory, it was hypothesized that the target P3 complex would be elicited by multiple context updating operations, namely, by the updating of surprising sensory units (as evidenced by observing between-conditions differences in P3-like positivities in the S cluster), the updating of motor units (R cluster), or the updating of intermediate sensorimotor units (C cluster). Further, the scalp topographies of these positivities were expected to differ subtly between task conditions, with more frontally distributed scalp topographies for the most informative flanker stimuli (Fig. 1b, Table 1). Based on the earlier latency of the frontal target N2 component, and its role in conflict detection, task effects were mostly predicted for the stimulus-locked cluster, as a previous stage for subsequent context updating indexed by target P3-like activity.

Method

Participants

The current study combined the adult participants of two previous studies (n = 12 from Brydges et al. 2012; n = 13 from Brydges et al. 2013), plus previously unpublished data from 20 more participants. In total, 45 undergraduate psychology students (M_{age} = 21.93 years, SD_{age} = 6.30 years, range = 18–49 years); 26 females and 19 males; 37 right-handed and 8 left-handed) were recruited for the study. All participants self-reported normal or corrected-to-normal vision, no history of color blindness or neurological disorders, and each participant performed above chance on all three task conditions. The samples were combined in order to increase statistical power given that neuroscientific studies are commonly underpowered (Button et al. 2013). The current hypotheses were only tested on the entire sample and not on the previously published samples.

Materials

The same hybrid go/nogo flanker task used by Brydges et al. (2012, 2013) was used in this study. Each stimulus consisted of five fish presented on a blue background. An arrow on the body of the fish specified direction and the target was the central fish. Participants were instructed to press a response button on a keyboard (red felt patches on the 'Z' and '/' keys of a QWERTY keyboard) analogous to the direction of the central fish. The task had three conditions: in the congruent condition (.5 probability), the fish were green and all facing the same direction (.25 probability for left and right facing green fish, respectively). In the incongruent condition (.25 probability), the fish were also green, however the flankers faced the opposite direction to the central target (with .125 probability of left and right incongruent flankers, respectively). In the nogo condition (.25 probability), the fish were congruent and red (again with .125 probability of either left or right facing red fish), and participants were required to withhold their response. Each fish subtended .9° horizontally and .6° vertically, with .2° separating each fish (see Fig. 2). A fixation cross was presented in the centre of the computer screen for 500 ms before the stimulus appeared immediately above it. Stimuli were presented in random order for 300 ms with a 2000 ms inter-stimulus interval. The task

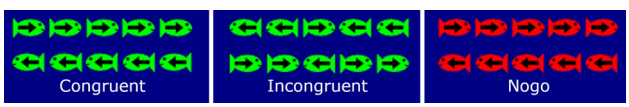

Fig. 2 The six stimuli used in the current study

was presented to the participants as a game in which they should feed the central fish. Speed and accuracy were equally emphasized. Eight practice trials were administered to ensure the participants understood the task requirements. A total of 176 trials were subsequently presented in one block.

Information theoretical estimations

We adopted an information theoretical model of cognitive control as a formal tool to help us operationalize the task context in terms of low- and high-order sensorimotor (S–R) information transmission within a putative hierarchy of fronto-parietal control processes (Fig. 1a; cf. Barceló and Knight 2007; Barceló and Cooper 2018a). In doing so, we followed recommendations by Miller (1956) for estimating the amount of information transmitted between contextually related stimuli and responses. These estimates allowed us to define the informational structure of our flanker task in terms of, not only mean stimulus probabilities, but also joint probabilities among stimuli, their associated motor responses, and any relevant cognitive control operation putatively involved (e.g., updating of high-order hidden units; Fig. 1a). Thus, the task context was modelled at two hierarchically distinct levels: (1) low-order sensorimotor S–R links, and (2) hypothetical high-order hidden units (Miller and Cohen 2001; Friston et al. 2017). Accordingly, the working memory representation of congruent green flanker targets and their associated responses (i.e., the low-order s_i-r_j links in Fig. 1a) was to be twice as frequently activated compared to the working memory representation of incongruent green flanker targets, or that of red nogo distracters. Importantly, the dynamic engagement of prefrontal resources on a trial-by-trial basis was hypothesized to depend on the number of high-order 'hidden' units necessary for regulating the dynamic updating of the six low-order sensorimotor units being held at posterior association cortices, with a larger number of high-order hidden units involving greater allocation of prefrontal resources (Fig. 1b; cf. Friston et al. 2017). Thus, whereas one high-order hidden unit implies no transmission of information through prefrontal cortices, three high-order hidden units involve an averaged transmission of 5.0 bits of information (Table 1). Models considering different high-order hidden units for left and right stimuli and responses were dismissed as implausible, given evidence of similar target N2 and P3 responses irrespective of the left versus right direction of flanker stimuli. Note that these information estimates can be seen as a more formal and accurate way to translate into bits the mean probabilities of task events, as is common practice in most experimental psychology studies. Yet they provide a common metric to compare different task conditions at both low- and high-order levels in the putative hierarchy of cognitive control. For instance, instead of saying that a left green congruent target occurs with an overall mean probability of $p = .25$ in our flanker task, we chose to quantify this in bits by saying that the sensory entropy of this trial type is: $H(s_1) = -.25 \cdot \log_2 .25 = .50$ bits. A similar formalism was used to quantify in bits the relative probabilities of the six specific low-order s_i-r_j links, and the hidden high-order s_i-ts_k links, using the concept of transmitted information: $I(s_i, r_j) = \log_2 p(s_i, r_j) - \log_2 p(s_i) - \log_2 p(r_j)$ and $I(s_i, ts_k) = \log_2 p(s_i, ts_k) - \log_2 p(s_i) - \log_2 p(ts_k)$ for low- and high-order levels in the hierarchy of control, respectively (Fig. 1a; cf. Miller 1956). Table 1 offers a summary of these information-theoretic estimations; for a more detailed technical description, see the Supplementary material (cf. Barceló and Cooper 2018a).

Electrophysiological acquisition

The EEG was continuously recorded using an Easy-Cap™. Ag/AgCl sintered ring electrodes were placed at 33 sites based on Easy-Cap montage 24. Eye movements were measured with bipolar leads placed above and below the left eye. The EEG was amplified with a NuAmps 40-channel amplifier, and digitized at a sampling rate of 250 Hz. Impedances were below 5 kΩ prior to recording. During recording, the ground lead was located at AFz and the right mastoid was set as reference.

EEG data were processed using MATLAB (Mathworks, Navick, MA) through a pipeline utilizing EEGLAB version 14..0 (Delorme and Makeig 2004), ERPLAB version 6.1.3 (Lopez-Calderon and Luck 2014) and ADJUST version 1.1.1 (Mognon et al. 2011). Preprocessing was performed in EEGLAB by re-referencing offline to a common average, and bandpass filtering the data (.1–30 Hz). Epochs for each stimulus type were extracted from 100 prestimulus to 1000 ms poststimulus onset. Independent components analysis was conducted using the extended infomax algorithm (Bell and Sejnowski 1995), and ADJUST was used to detect any artefactual components (including blinks, horizontal and vertical eye movements, and muscle movement). These components were removed, and the remaining components were back-projected to the electrode space. The mean number of components removed per participant was 6.67 ($SD = 3.36$). Epochs containing EEG signals exceeding ± 100 μV at any electrode site were excluded from analyses.

RIDE

RIDE analysis followed the methods described in Ouyang et al. (2011, 2015). The RIDE toolbox and manual can be found at http://cns.hkbu.edu.hk/RIDE.htm. RIDE

decomposes ERPs into stimulus-locked, response-locked, and central clusters (terms S, R, and C, respectively, from here), though for the nogo condition, no R cluster was extracted as a correct nogo trial requires no response to be made (Ouyang et al. 2013). The latency estimates of S and R (L_S and L_R) were obtained from the stimulus onset to 300 ms post-stimulus onset, and from 200 pre-response to 200 ms post-response, respectively. The latency estimate of C (L_C) is derived from the data of each individual participant using the following iterative process.

Initial estimation of L_C

RIDE separates component clusters by estimating the latency of the S, C, and R clusters on single trials. It is assumed that the C cluster is not stimulus or response-locked, and that L_C is variable over single trials as a result of this. Based on L_S, L_C, and L_R, the evoked potentials of S, C, and R are dissociated from one another in later steps. The decomposition module makes use of both external time markers (e.g., stimulus and response onset) and estimated component latencies. The latency-locked clusters (i.e., S and R clusters) are removed from the single-trial data before the latency-variable component cluster (the C cluster) is estimated. An initial estimation of L_C was made with the Woody (1967) filter for each recording site between 250 and 550 ms. The mean latency across channels was taken as L_C across the scalp (for further technical details see Ouyang et al. 2011, 2015).

Statistical analyses

For both traditional ERP and RIDE analyses, 3 × 2 repeated measures ANOVAs were conducted on the data to identify mean differences in amplitude between conditions (congruent, incongruent, and nogo) and electrode site (Fz and Pz). These electrode sites were chosen based on Brydges and Barceló (2018). For the ERP analyses, mean amplitudes were analyzed between 220 and 270 ms (corresponding to the N2 component), 300–400 ms (P3), 450–550 ms (LPC_1), and 600–700 ms (LPC_2). These latency windows were chosen based on previous N2 and target P3 research (e.g., Barceló and Cooper 2018a; Falkenstein et al. 1999) and visual inspection of the grand mean ERP waveforms. Peak-to-peak N2-P3 amplitudes were also measured to clarify the sign of congruency effects at frontal regions (Folstein and Van Petten 2008). To ensure consistency, these same time windows were used in the RIDE analyses: the 220–270 ms and 300–400 ms were extracted from the S cluster, and the 300–400 ms, 450–550 ms, and 600–700 ms windows were extracted from the C cluster. This also follows the procedures applied by previous research using RIDE (e.g., Ouyang et al. 2011; Verleger et al. 2014). Additionally, the R cluster was defined as the mean amplitude occurring 50 ms before a correct response was made, to 50 ms after the response, following Brydges and Barceló (2018). As mentioned previously, no R cluster was extracted for the nogo condition as a correct trial requires no response to be made, and hence, the statistical design was a 2 (site) × 2 (condition) repeated measures ANOVA. Additionally, a repeated measures ANOVA with condition as the only factor was conducted on the behavioral accuracy data, and a paired-samples *t* test was conducted on the mean RTs for the congruent and incongruent conditions.

In addition to traditional null hypothesis significance testing, we conducted Bayesian analyses (Keysers et al. 2020; Wagenmakers 2007; Wagenmakers et al. 2018). Bayesian statistics are advantageous over frequentist statistics for various reasons: first, Bayesian analyses allow a hypothesis to be accepted or rejected by gathering evidence in favor of it (Dienes 2011; Kruschke 2013). That is, the alternative hypothesis can only be falsified by accepting the null hypothesis over it, which Bayesian statistics allow for. Second, Bayesian statistics allow the same data points to be repeatedly tested without researchers having to precommit to a specified sample size, whereas this cannot be done with frequentist statistics (Armitage et al. 1969). Third, Bayesian statistics are produced in terms of the probability of hypotheses given data, as opposed to data given hypotheses (Cohen 1994). Bayesian statistics are more interpretable than frequentist statistics (Dienes 2011; Kruschke 2013), and assess the credibility of one hypothesis compared to another. Hence, Bayesian methods are well-suited for testing hypotheses about which of the three models presented in Table 1 and Fig. 1b best explains ERP and RIDE data at frontal regions, particularly in order to counteract potential Type I errors associated with *p* values of conventional frequentist statistics (Luck and Gaspelin 2017). A Bayes Factor (BF) was calculated from the Bayesian ANOVAs to test how much the data supported the alternative (H1) over the null (H0) hypothesis (that is, how strong the evidence was in favor of one model over another), using a an *r* scale with a width of .50 for fixed effects. Based on guidelines set by Jeffreys (1961), a $BF_{10} > 3$ was considered sufficient evidence in favor of the alternative hypothesis, and a $BF_{10} > 10$ was considered to be strong evidence in favor. Of note, BF_{10} refers to the BF value of H1 being supported over H0, whereas BF_{01} refers to the opposite. To calculate BF_{01}, one simply inverts the BF_{10} value. Additionally, posterior probabilities (henceforth referred to as $p(H|D)$) evaluated the probability of a hypothesis being correct given the observed data, with values of .50-.75, .75-.95, .95-.99, and > .99 indicating weak, positive, strong, and very strong evidence in favor of the alternate hypothesis, respectively (Masson 2011;

Raferty 1995). Alternative hypotheses would only be accepted if $BF_{10} > 3$. Both the frequentist and Bayesian analyses were conducted using JASP version .8.5.1 (JASP Team 2018; Brydges and Gaeta 2019). To save space, simple effects of the frequentist ANOVA for Fz are only reported when they differ from the results of Bayesian analyses.

Results

Behavioral results

Descriptive statistics of the behavioral data are presented in Table 2. A repeated measures ANOVA found a main effect of condition on accuracy ($F(2,88) = 72.98$, $p < .001$, $\eta_p^2 = .62$), and subsequent post hoc paired-samples t-tests found lower accuracy on the incongruent condition than the congruent and nogo conditions (congruent-incongruent $t(44) = 9.83$, $p < .001$, Cohen's $d = 1.99$; congruent-nogo $t(44) = 1.59$, $p = .12$, Cohen's $d = .26$; nogo-incongruent $t(44) = 8.44$, $p < .001$, Cohen's $d = 1.37$). Also, mean RTs were longer in the incongruent condition compared to the congruent condition ($t(44) = 15.80$, $p < .001$, Cohen's $d = 1.19$).

Conventional ERP analyses

Figure 3 shows the grand average ERP waveforms for the three conditions at Fz and Pz sites, and mean amplitude scalp maps corresponding to five time windows in the recording epoch, corresponding to the N2, P3, LPC_1, and LPC_2 components. To aid comparison between conventional ERP components and RIDE clusters, Table 3 presents a summary of the main effects and interactions for the site and condition factors; however, for the sake of brevity, only those interactions, main effects, and post hoc tests that are of theoretical importance are described in-text below.

N2 (220–270 ms)

The site × condition interaction was not significant, whereas the main effects of condition and site both reached

Table 2 Descriptive statistics of behavioral results (means, with standard deviations in parentheses)

Condition	Reaction time (ms)	Accuracy (proportion correct)
Congruent	378 (43)	.98 (.03)
Incongruent	447 (60)	.82 (.11)
Nogo	N/A	.96 (.06)

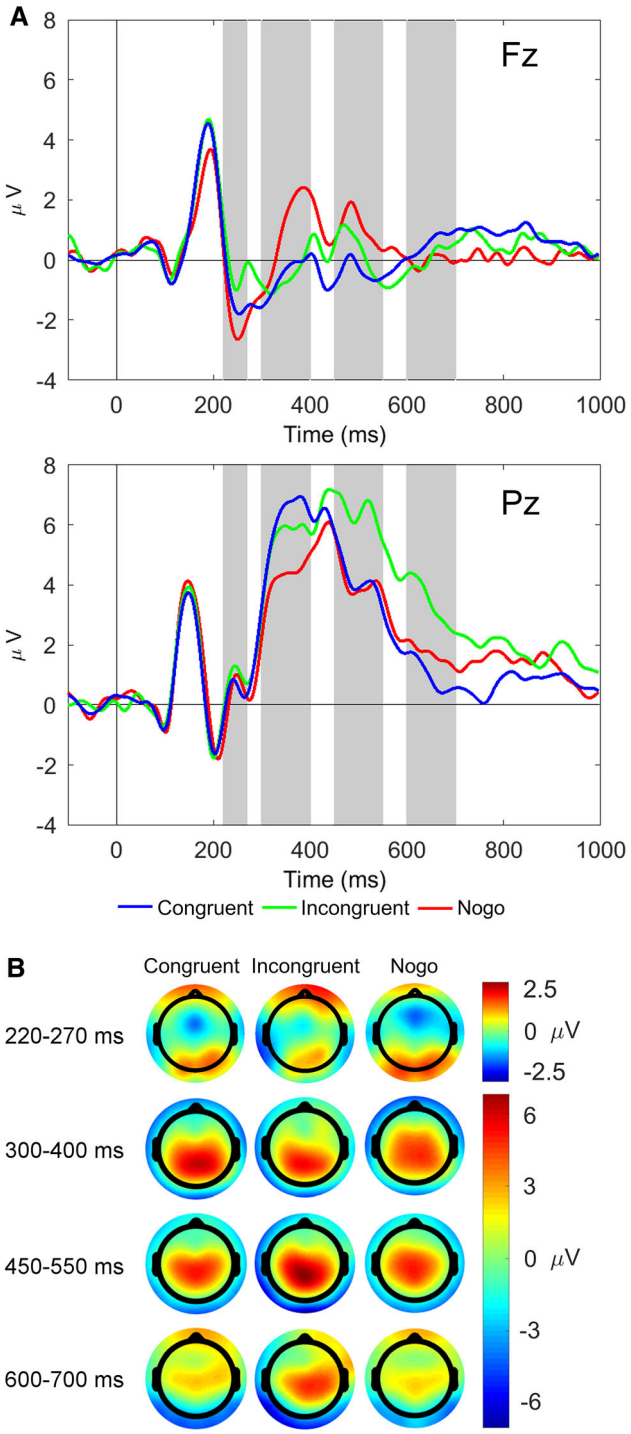

Fig. 3 Stimulus-locked grand average ERP waveforms and scalp topography maps. **a** Waveforms depict mean voltages recorded from Fz (top) and Pz (bottom). Shaded areas indicate time windows used to measure mean ERP amplitudes tracking the temporal dynamics of the N2 and late P3-like complex: N2 (220–270 ms), P3 (300–400 ms), LPC_1 (450–550 ms), and LPC_2 (600–700). **b** Scalp topographies of the N2 and three late P3-like positivities depicted in **a** across task conditions (i.e., congruent, incongruent, and nogo)

Table 3 Summary of ANOVA results showing task effects for conventional ERP components and the RIDE decomposed C, S and R clusters

	Site *df* 1, 44		Condition *df* 1, 44		Site x condition *df* 2, 88	
	F	η^2	*F*	η^2	*F*	η^2
ERPs						
N2 (220–270 ms)	6.52*	.13	8.75***	.17	2.30 *ns*	.05
P3 (300–400 ms)	55.35***	.56	.72 *ns*	.02	21.35***	.33
LPC_1 (450–550 ms)	61.44***	.58	13.23***	.23	9.90***	.18
LPC_2 (600–700 ms)	7.72**	.15	4.23*	.09	8.81***	.17
RIDE S cluster						
sN2	.99 *ns*	.02	10.81***	.20	5.76**	.12
sP3	6.56*	.13	3.98*	.08	3.34*	.07
RIDE C cluster						
cP3	41.24***	.48	6.78**	.13	1.96 *ns*	.04
$cLPC_1$	36.20***	.45	10.76***	.20	1.05 *ns*	.02
$cLPC_2$	7.33**	.14	3.59*	.08	2.67 *ns*	.06
RIDE R cluster						
rP3	83.19***	.65	1.54 *ns*	.03	6.33*	.13

ns non-significant, * $p < .05$, ** $p < .01$, *** $p < .001$. The *df* values for the R cluster interaction were 1, 44

significance (see Table 3). Bayesian analyses at Fz found evidence in favor of a difference between conditions (BF_{10} = 93.50, p(H|D) = .99), with post hoc tests finding evidence in favor of a smaller (less negative) incongruent N2 than the congruent (BF_{10} = 9.51) and nogo conditions (BF_{10} = 27.87), which did not differ between each other (BF_{10} = .88).

P3 (300–400 ms)

The site × condition interaction and the main effect of site were both significant, whereas the main effect of condition was not (Table 3). Post-hoc *t*-tests found larger mean P3 amplitudes in the nogo condition than in the congruent and incongruent conditions at Fz ($t(44) = 4.24$, $p < .001$, and $t(44) = 3.14$, $p = .003$, respectively), with the reverse being true at Pz ($t(44) = -5.26$, $p < .001$, and $t(44) = -3.25$, $p = .002$, respectively). Bayesian analyses at Fz found evidence in favor of a difference between conditions (BF_{10} = 177.06, p(H|D) > .99), with the nogo P3 being larger than the congruent (BF_{10} = 211.36) and incongruent conditions (BF_{10} = 11.08), which did not differ between them (BF_{10} = .16).

LPC_1 (450–550 ms)

The site × condition interaction was significant, as were the main effects of site and condition (Table 3). Paired-samples *t*-tests found that the incongruent and nogo conditions elicited larger LPC_1 amplitudes than the congruent condition at Fz ($t(44) = 2.25$, $p = .029$, and $t(44) = 3.93$, $p < .001$, respectively). At Pz, however, the incongruent condition evoked larger LPC_1 amplitudes than the congruent and nogo conditions ($t(44) = 4.81$, $p < .001$, and $t(44) = 4.30$, $p < .001$, respectively). Bayesian analyses at Fz found evidence in favor of a difference between conditions (BF_{10} = 20.33, p(H|D) = .95), with the nogo LPC_1 being larger than the congruent (BF_{10} = 87.24). The evidence for/against differences between congruent and incongruent LPC_1, and incongruent and nogo LPC_1 was weak (BF_{10} = 1.58 and BF_{10} = .52, respectively).

LPC_2 (600–700 ms)

The site × condition interaction was significant, as were the main effects of site and condition (Table 3). Paired-samples *t*-tests found that the incongruent condition evoked larger mean LPC_2 amplitudes than both the congruent and nogo conditions at Pz ($t(44) = 6.05$, $p < .001$, and $t(44) = 2.45$, $p = .018$, respectively). Bayesian analyses at Fz found evidence against a difference in LPC_2 between conditions (BF_{10} = .16, p(H|D) = .14).

RIDE analyses

Waveforms and scalp maps for the S, C, and R clusters are displayed in Figs. 4, 5 and 6, respectively. The S cluster appears to reflect mostly early sensory and attentional processes at stimulus onset. In the C cluster, the nogo condition elicits a large central P3-like positivity, whereas

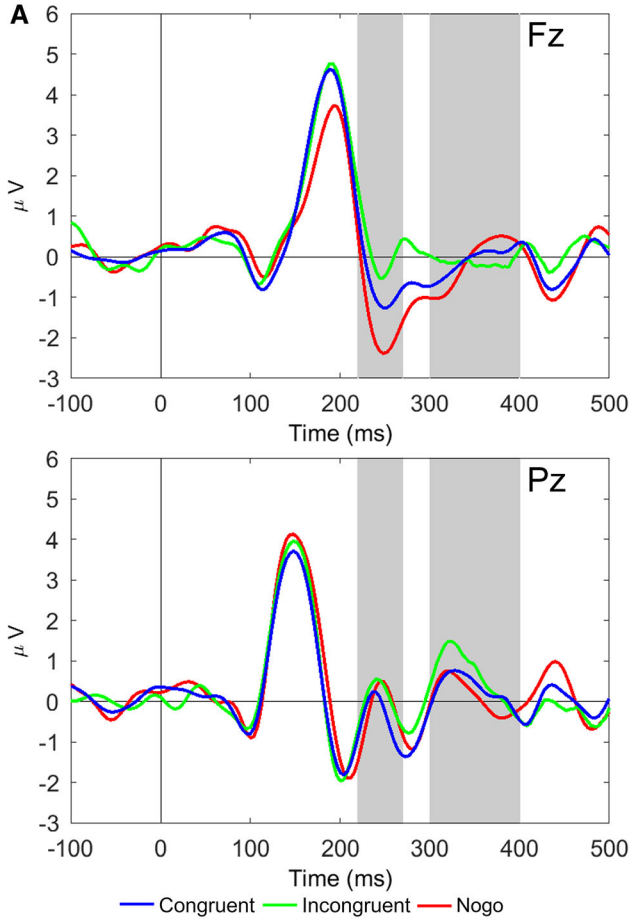

Fig. 4 Stimulus-locked waveforms and scalp maps for the S cluster. **a** Waveforms depict grand-averages recorded from Fz (top) and Pz (bottom). The shaded area is the latency window used to measure P3-like activity in the S cluster: sN2 (220–270 ms), and sP3 (300–350 ms). **b** Scalp topographies for each task condition are mean amplitudes within the shaded time window in the waveforms

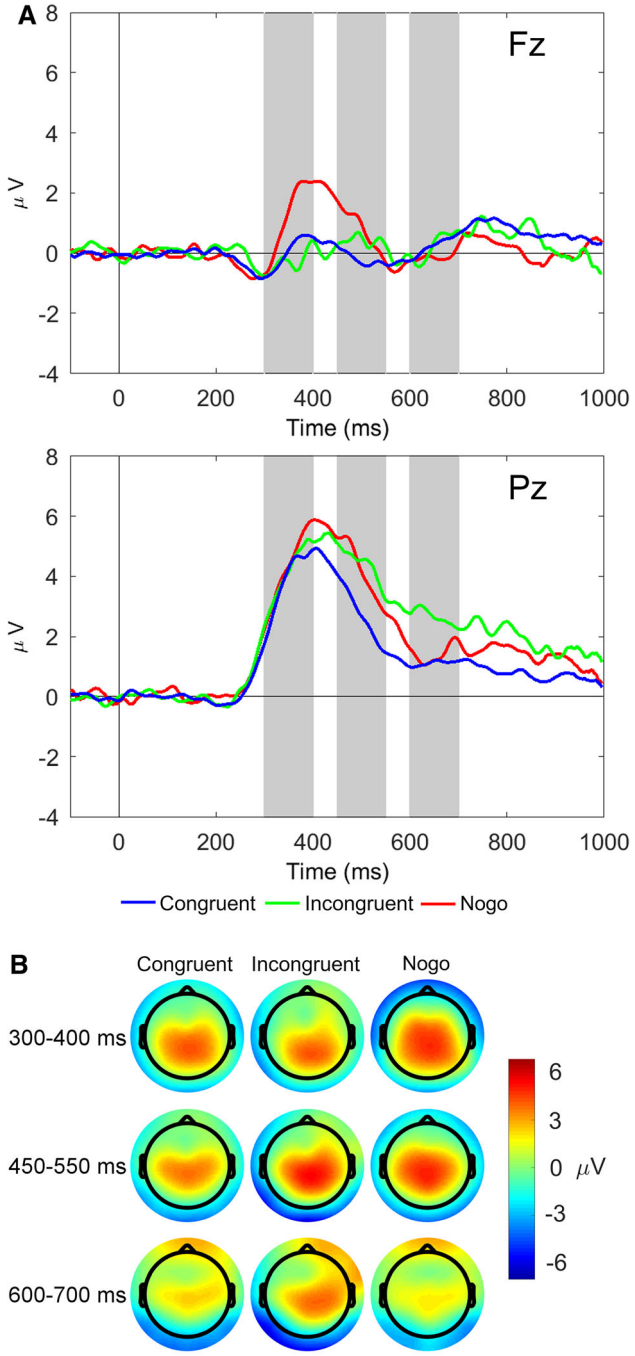

Fig. 5 Latency-variable C cluster waveforms and scalp topography maps. **a** Waveforms depict mean voltages recorded from Fz (top) and Pz (bottom). Shaded areas indicate time windows used to measure mean amplitudes tracking the temporal dynamics of the C cluster P3-like complex: cP3 (300–400 ms), $cLPC_1$ (450–550 ms), and $cLPC_2$ (600–700 ms). **b** Scalp topographies of the three late cP3-like positivities depicted in **a** across task conditions (i.e., congruent, incongruent, and nogo)

the incongruent condition elicits a flatter P3/LPC-like centro-parietal complex. In the R cluster, the positive parietal peaks are closely associated with response time, as expected, with an additional frontal peak elicited by the incongruent trials. A summary of the simple effects for the Bayesian analyses at the Fz site is presented in Table 4.

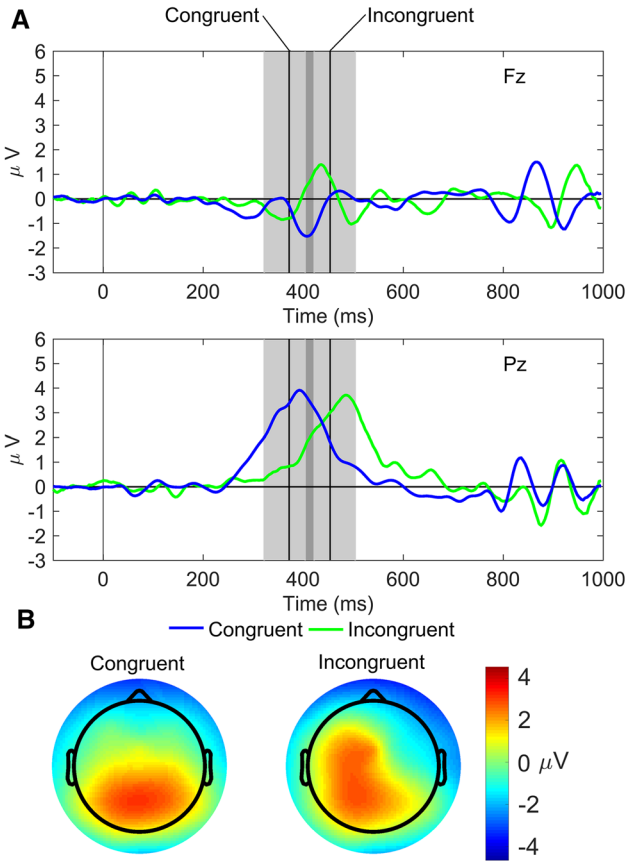

Fig. 6 Response-locked waveforms and scalp maps for the R cluster. **a** Waveforms depict grand-averages recorded from Fz (top) and Pz (bottom). Black vertical lines indicate the median response time for each task condition and shaded area is the latency window used to measure P3-like activity in the R cluster (50 ms pre-response to 50 ms post response). **b** Scalp topographies for each task condition are the mean amplitudes measured in a 50 ms pre-response to 50 ms post response time window around the median response time for each condition

S cluster

For the sN2 component, the site × condition interaction and the main effect of condition were both significant (Table 3). Paired-samples *t*-tests found that mean sN2 amplitudes elicited by the nogo condition were larger (more negative) at Fz than at Pz ($t(44) = 2.12$, $p = .040$). Bayesian analyses at Fz found evidence for differences between conditions ($BF_{10} = 2987.04$, $p(H|D) > .99$), revealing strong evidence for differences between all conditions (nogo > congruent > incongruent, where '>' indicates more negative; nogo-congruent $BF_{10} = 6.42$; nogo-incongruent $BF_{10} = 295.30$; congruent-incongruent $BF_{10} = 10.54$).

For the sP3 component, both main effects and the site × condition interaction were significant (Table 3). Paired-samples *t*–tests found that sP3 amplitude at Pz was larger in the incongruent condition than both in the congruent ($t(44) = 2.49$, $p = .017$) and the nogo conditions ($t(44) = 3.37$, $p = .002$). Bayesian analyses at Fz found evidence against a difference between any conditions ($BF_{10} = .07$, $p(H|D) = .07$) for mean N2 amplitudes. In turn, when considering peak-to-peak N2-P3 amplitudes at Fz, Bayesian analyses found moderate evidence in favor of differences between conditions ($BF_{10} = 3.67$, $p(H|D) = .79$), with the nogo N2-P3 being larger than the congruent N2-P3 ($BF_{10} = 56.90$); with weak evidence for/against differences between incongruent and nogo N2-P3 peak-to-peak amplitudes ($BF_{10} = .59$).

C cluster

For the cP3 component, the site × condition interaction was not significant, whereas there were main effects of site and condition (see Table 3). Post-hoc tests showed that cP3 amplitude was maximal at Pz in comparison to Fz ($t(44) = 6.42$, $p < .001$), and the cP3 amplitude was larger for nogo than congruent and incongruent conditions ($t(44) = 3.29$, $p = .002$, and $t(44) = 2.71$, $p = .010$), respectively). Bayesian analyses at Fz found evidence in favor of a difference between conditions ($BF_{10} = 13.72$, $p(H|D) = .93$), showing evidence for differences between nogo and the other two conditions (nogo-congruent $BF_{10} = 11.53$; nogo-incongruent $BF_{10} = 4.65$).

For the $cLPC_1$ component, the site × condition interaction was not significant, but the main effects of site and condition both reached significance (Table 3). Maximal

Table 4 Summary of simple effects for Bayesian analyses at the Fz site

Time window	ERPs	S cluster	C cluster	R cluster
N2 (220–270 ms)	N = C > I	N > C > I (3)	–	–
P3 (300–400 ms)	N > C = I	N = C = I (1)	N > C = I (2)	C < I (3)
LPC_1 (450–550 ms)	N > C = I	–	N = C = I (1)	–
LPC_2 (600–700 ms)	N = C = I	–	N = C = I (1)	–

N nogo trials, *C* congruent trials, *I* incongruent trials. Values in parentheses next to RIDE clusters indicate the models that are best supported by the findings (1 = model 1; 2 = model 2; 3 = model 3). No differences between task conditions lend support to model 1 (i.e., N = I = C), whereas significant differences between all task conditions lend support to model 3 (i.e., N > I > C; see Fig. 1b)

$cLPC_1$ amplitude was found at Pz in comparison to Fz ($t(44) = 6.02$, $p < .001$), and the $cLPC_1$ amplitude was larger for the incongruent and nogo stimuli than the congruent stimuli ($t(44) = 3.76$, $p = .001$, and $t(44) = 3.05$, $p = .004$), respectively). Bayesian analyses at Fz found weak evidence against differences between conditions ($BF_{10} = .70$, $p(H|D) = .41$).

For the $cLPC_2$ component, the site × condition interaction was not significant, with significant main effects for site and condition (Table 3). Paired-samples *t*-tests showed that the mean amplitude was larger at Pz than Fz ($t(44) = 2.71$, $p = .010$), and that the cLPC2 amplitude elicited by the incongruent stimuli was larger than the congruent stimuli ($t(44) = 2.92$, $p = .006$). Bayesian analyses at Fz found evidence against differences between conditions ($BF_{10} = .11$, $p(H|D) = .10$).

R cluster

The R cluster time window was 50 ms pre-response to 50 ms post-response for the congruent and incongruent conditions. The interaction and main effect of site reached significance (Table 3). Paired-samples *t*-tests found larger mean rP3 amplitudes in the incongruent than in the congruent condition at Fz ($t(44) = 2.67$, $p = .011$), while no such a difference was apparent at Pz ($t(44) = 1.05$, $p = .30$). Bayesian analyses at Fz also found evidence in favor of a difference between congruent and incongruent conditions ($BF_{10} = 4.26$, $p(H|D) = .81$).

Finally, in light of the conspicuous differences in peak rP3 latency between conditions observed at Pz, a paired-samples *t*-test was conducted, which indicated that such differences were significant ($t(44) = 8.93$, $p < .001$, Cohen's $d = 1.33$).

Brain-behavior correlations

Lastly, Pearson product-moment linear correlations between RIDE decomposed amplitudes and behavioral measures (mean RTs, accuracy, and incongruency costs) were conducted. No correlations reached statistical significance (following Bonferroni correction). Additionally, in the light of the conspicuous differences in peak rP3 latency observed between congruent and incongruent trials, one final correlation was conducted between within-subjects differences in mean RT and the peak latency of the rP3 between those conditions. That correlation was statistically significant ($r = .32$, $p = .033$), with the scatterplot displaying a linear relationship (see Fig. 7).

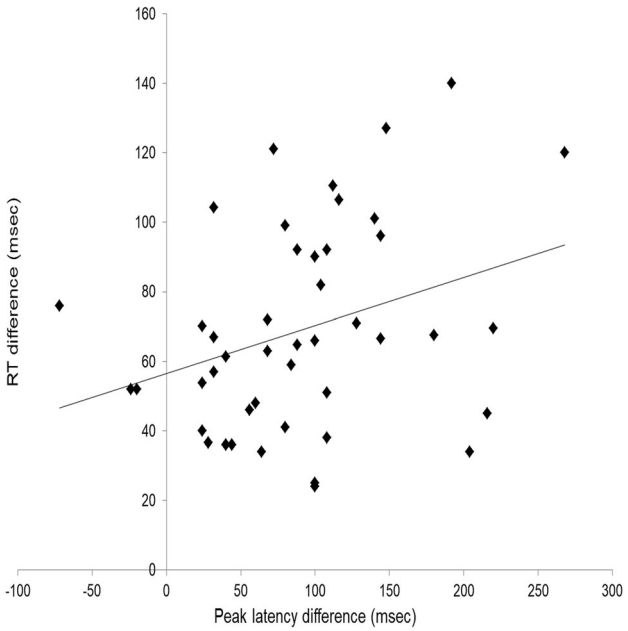

Fig. 7 Scatterplot of within-subject difference in peak rP3 latency (msec; congruent subtracted from incongruent trials) and difference in mean reaction time (msec; congruent subtracted from incongruent trials)

Discussion

The current study aimed to expand upon Barceló and Cooper's (2018a) and Brydges and Barceló's (2018) RIDE decomposition of target P3-like positivities during cognitive control of task switching, by examining these components in a flanker task. Based on our information theory estimates (Table 1), it was hypothesized that target (congruent and incongruent) and non-target (nogo) trials in the flanker task would elicit frontal N2 and P3 activity indexing conflict detection and context updating operations that could be decomposed into stimulus-locked, intermediate, and response-locked sub-components. The amplitudes and scalp topographies of the N2-P3 complex were expected to be modulated by dynamic trial-by-trial adjustments in information processing demands, with larger frontal N2 and P3 amplitudes expected for task conditions posing larger cognitive demands (Fig. 1b; cf. Miller 1956). More specifically, we examined whether evidence for one, two or three high-order hidden units (or latent variables) could be identified in our flanker task in line with a well-known model of prefrontal executive control (Table 1; Fig. 1a; Miller and Cohen 2001). The results showed a highly dynamic picture of effects, with a stimulus-locked frontal N2 revealing early sensory conflict detection and fast categorization of all three trial types, resulting in subsequent frontal P3-like activity (high-order context updating) elicited by the highly informative nogo trials (C cluster) and by the cognitively demanding

incongruent trials (R cluster). In turn, and as predicted by model 3 in Fig. 1b, the least informative congruent trials did not elicit frontal P3-like activity, although all three trial types did elicit parietally distributed P3-like activity (low-order context updating), mostly within the C cluster. These novel findings support the presence of at least three distinct high-order hidden units momentarily regulating performance in our flanker task (Fig. 1), as indexed by split-second, dynamic information transmission across frontal and parietal scalp regions. Further, our findings provide the first evidence that behavioral congruency effects are directly related to delayed response-locked peak rP3 latencies in incongruent trials (cf. Figs. 6, 7), which in turn results from accumulative congruency effects observed earlier in the S- and C-clusters, as is further discussed in more detail below.

Based on predictions from model 3 in Fig. 1, it was hypothesized that the nogo and incongruent trials of our flanker task would require larger degree of cognitive control and engage more prefrontal resources than the congruent condition, in line with the differential amounts of contextual information being transmitted by each of those trial conditions (Fig. 1b; Table 1). Under the assumption that dynamic trial-by-trial changes in cognitive demands associated with different flanker stimuli can be modelled as information transmission through hypothetical high-order hidden units (Barceló and Cooper 2018b; Friston et al. 2017; Parr et al. 2020), we predicted task differences on the electrophysiological indexes of conflict detection (frontal N2) and context updating (fronto-parietal P3) depending on the putative number of high-order hidden units regulating performance of this hybrid go/nogo flanker task (Fig. 1a, b; Table 1; see Supplementary materials). As such, it was expected that larger amplitudes of the frontal N2 and fronto-parietal P3 components will be associated with a larger number of high-order hidden units involved. Our conventional ERP results were generally consistent with previous studies, although these necessarily represent a compound mixture of different component processes. Thus, we found that the classic P3 was enhanced at Fz for the highly informative nogo trials compared to congruent and incongruent trials, and the nogo-P3 was smaller over parietal regions (Fig. 3), in line with previous research (e.g., Gajewski and Falkenstein 2013). Both nogo and incongruent trials elicited larger frontal LPC_1 amplitudes than congruent trials, with incongruent trials eliciting significantly larger amplitude at Pz as well, consistent with previous research examining the LPC and task difficulty (Brydges et al. 2014). Now, in the light of our novel RIDE findings, these conventional target-P3 and nogo-P3 effects can be reinterpreted as a combination of stimulus-locked, response-locked, and latency-variable P3-like component processes.

Importantly, our novel RIDE results help clarify the functional significance of distinct component operations tracked by the frontal N2 and fronto-parietal P3-like modulations observed in all three clusters (Folstein and Van Petten 2008; Kałamała et al. 2018). In line with Brydges and Barceló's (2018) findings, the largest P3-like modulations were captured by the C cluster, which is likely to index higher-order control operations, such as updating of high-order response policies given the sensory information and probability of the incoming stimuli (i.e., frequent green fish vs. infrequent red fish). Interestingly, the S cluster captured not only early stimulus-locked peaks (i.e., a P2-like peak at both frontal and parietal sites between 140 and 200 ms), but also revealed frontal N2 and parietal P3-like activity putatively indexing both high- and low-order transfer of information respectively from early perceptual conflict detection to context updating triggered by changes in visual stimulation, since task condition also modulated the parietal sP3 (i.e., low-order context updating; see Fig. 4). From the context updating theory of the P3 (Donchin and Coles 1988), this implies that changes in the perceptual aspects of the environment may trigger context updating at both high-order (Fz) and low-order (Pz) levels in the hierarchy of cognitive control, which was the case for our highly informative nogo and incongruent trials, respectively, as predicted by model 3 in Fig. 1b. There was also a visible response-locked P3-like component (rP3) with maximal parietal scalp distribution, likely reflecting "context updating" operations elicited by changes in motor or premotor control units associated with trial-by-trial variability in response selection. Importantly, and consistent with predictions from model 3, the more cognitively demanding incongruent condition elicited a significantly larger frontal rP3 and this peaked later over parietal regions than the easier congruent condition (cf. Brydges and Barceló 2018). This suggests that the low-level S–R mapping for congruent trials was easier to implement because it was more probable and thus might have been naturally adopted as the default stimulus–response mode. In turn, in order to implement the correct S–R mapping for infrequent incongruent trials, participants must effortfully select the contextually isolated central target and then reverse the default S–R mapping, which presumably delayed the peak latency of parietal rP3 component downstream. Overall, these results support the findings of Brydges and Barceló (2018), in that changes in sensory, motor and sensorimotor levels of representation in the hierarchy of cognitive control can all trigger context updating mechanisms that differentially engage fronto-parietal regions from 220 to 700 ms post-stimulus onset and beyond, possibly reflecting temporarily recurrent activation of various nodes across the fronto-parietal network in those more informative task conditions engaging larger cognitive demands (i.e., nogo and

incongruent trials; Bledowski et al. 2004; Duncan 2010; cf., Johnson and Donchin 1985).

Stimulus-locked activity

In the S cluster, frontal sN2 amplitude was modulated by task condition (nogo > congruent > incongruent; with nogo being most negative). Bayesian analyses provided evidence of differences in frontal sN2 amplitude between all three conditions, implying that conflict detection is a stimulus-locked process that momentarily involved three distinct high-order hidden units being held at prefrontal cortices (cf. model 3 in Fig. 1b), and has been putatively associated to the anterior cingulate cortex (Botvinick et al. 2004; Carter and van Veen 2007; Fan 2014; van Veen and Carter 2002). Mean frontal sN2 amplitudes were smaller for incongruent than congruent trials, an inconsistent result that could be attributed to our nogo version of the flanker task, since nogo trials affect the probability of other trials, and the participant's overall strategy of conflict resolution (Kałamała et al. 2018). Therefore, the low probability of red nogo trials in our version of the flanker task may have influenced the participant's overall strategy of conflict resolution. Such an explanation is supported by our formal estimation of information transmission between stimuli and responses (including "nogo" responses) that identify nogo trials as the most informative trials in our study (Model 3; Fig. 1b). It should be noted that the information conveyed by incongruent trials would be larger than that of nogo trials if these were the most frequent trial condition (i.e., C = .25, I = .25; NoGo = .50; see Supplementary materials). Thus, our simple information theory model has heuristic value and can be used to make testable predictions to help understand the influence of trial probability on frontal N2-P3 congruency effects (Folstein and van Petten 2008). That is, the amount of conflict and context (belief) updating does not only depend on the labels assigned to the task conditions (i.e., congruent, incongruent, and nogo), but on the probabilistic structure of the task as can be best defined through the joint and conditional probabilities between task events, responses and intervening 'hidden' variables (Barceló and Cooper 2018b; Doya and Ishii 2007; Friston et al. 2017; Parr et al. 2020). In line with this interpretation, reduced frontal N2 in incongruent trials could be due to a small positive P3-like bump following the frontal N2 peak in incongruent trials (Fig. 3) that is more clearly visible in the S-cluster (Fig. 4). We quantified this positive bump by measuring peak-to-peak N2-P3 amplitudes within 200–300 ms post-stimulus (Folstein and van Petten 2008). Peak-to-peak N2-P3 amplitudes were largest for the most informative nogo and incongruent trials, and smallest for the least informative congruent trials, with no differences between nogo and incongruent trial conditions. This small positive peak might signal the moment when frontal cortex sends a signal downstream to revert the default congruent S–R mapping in the face of a highly informative incongruent trial. As a consequence, larger parietal sP3 amplitudes were elicited by incongruent trials than either congruent or nogo trials in the S cluster. This finding suggests that low-order context updating may be triggered by an infrequent visual target that differentially engages temporo-parietal regions of the fronto-parietal network to anticipate a change in response demands, thus enhancing parietal sP3 amplitudes on incongruent trials. Such low-order context updating may index an early stage of S–R remapping in the incongruent trials "to control for incorrect response preparation" (Folstein and Van Petten 2008). This finding suggests a highly dynamic and context-sensitive functioning of fronto-parietal networks, with fast split-second fluctuations in the amount of frontal and parietal resources engaged for processing each trial type (cf. Barceló and Cooper 2018a; Kieffaber and Hetrick 2005).

Additionally, the fact that the frontal N2 component elicited by the nogo condition was best captured by the S cluster rather than the C cluster suggests that what is traditionally considered the frontal nogo-N2 may largely reflect conflict detection triggered by stimulus-locked information transmission across prefrontal cortices (Carter and Van Veen 2007; Nieuwenhuis et al. 2004; Van Veen and Carter 2002). Specifically, the neural output of the frontal N2 may feed forward onto further high-order context updating operations (frontal P3), and even further down in the hierarchy of control into response inhibition and response selection operations at posterior association cortices (i.e., low-order context-updating; Fig. 1a), which could thus explain the modulations of subsequent processing stages captured by the latency variable and response-locked P3-like positivities (Botvinick et al. 2004; Gajewski et al. 2008). It should be acknowledged, however, that the frontal N2 component measured here could also potentially reflect response inhibition processes (e.g., Falkenstein et al. 1999), as opposed to conflict detection (Folstein and Van Petten 2008; Gratton et al. 2018). Yet, a compatible alternative is that our reversed congruency frontal N2 effect was a consequence of our unusual task design, using dissimilar 2:1 ratios of congruent to incongruent trials. Admittedly, this is a very unusual ratio, which might have led subjects to adopt a congruent mode of responding as a default. Then, in incongruent trials, subjects rapidly switched their response policies, resulting in the inhibition of the congruent rule rather than the inhibition of a congruent response. Indeed, our unusual results agree with a recent flanker task study showing reduced frontal N2 and enhanced frontal P3 during "rule inhibition", as compared to "response inhibition" or "flanker

inhibition" (Xie et al. 2017). It should also be noted that the ERP effects from task relevance and objective information are not well distinguished. One solution to distinguish these two factors is to use more probabilistic combinations to systematically reveal the impact of both (see Duncan-Johnson and Donchin 1977, for an example).

Latency-variable activity

In the central cluster, the cP3 peak (300–400 ms; the typical latency of classic P3 potentials) was modulated by high-order context updating, implying that the latency-variable cP3 was associated with updating of higher-order hidden units. Specifically, the Bayesian analyses on the cP3 component revealed the transient engagement of two high-order hidden units, one for updating to infrequent nogo S–R links and one for updating to target S–R links (i.e., thus supporting model 2 in Fig. 1b; Table 4). This was consistent with the frontal nogo cP3 to highly informative nogo trials requiring upholding a response, together with the absence of any frontal cP3 activity to the less informative target trials requiring a motor response (congruent and incongruent trials). In contrast, the $cLPC_1$ and $cLPC_2$ were not modulated by high-order context updating (i.e., there was moderate Bayesian evidence in favor of only one high-order hidden unit from Fz data, therefore supporting model 1 in Fig. 1b). Thus, both nogo and incongruent trials elicited greater $cLPC_1$ amplitudes than congruent trials over parietal regions, whereas incongruent trials continued eliciting greater parietal amplitudes than congruent trials in the $cLPC_2$ time window. These congruency effects over parietal regions in the non-phase locked C cluster suggest that cognitive control is a highly dynamic process, whereby once conflict is detected at frontal cortical regions (i.e., indexed by the frontal sN2 component), then context updating proceeds, first at high-order frontal regions (i.e., the nogo-cP3), and then later at low-order temporo-parietal association cortices ($cLPC_1$, $cLPC_2$) to update and reconfigure the S–R mappings needed to adaptively deal with different response demands. These findings suggest that the latency-variable components elicited in the C cluster capture several functionally distinct time-varying cognitive control operations resulting in subtly different P3-like scalp topographies as required by dynamic changes in cognitive demands (cf. Barceló and Cooper 2018a; Brydges and Barceló 2018).

Response-locked activity

In the response-locked cluster, a parietal P3-like positivity (rP3) showed a similar mean amplitude for congruent and incongruent trials, attesting for similar low-level context updating operations in both trial conditions. Most interestingly, though, there was an 80 ms difference in peak rP3 latency between conditions, suggesting that low-level context updating for incongruent trials was delayed regarding the comparatively easier congruent trials. This difference in parietal peak rP3 latency significantly correlated with behavioral reaction times, and is also consistent with predictions from model 3 in Fig. 1b, whereby only the highly informative incongruent trials demanding a reversal in S–R mappings elicited a frontal rP3 (high-order context updating) that influenced subsequent processes downstream by delaying the parietal rP3, an index of low-order S–R remapping (low-order context updating). Note that these more nuanced context updating operations are all response-locked and would thus remain hidden in conventional ERP waveforms (Fig. 3). This finding is similar to that reported by Brydges and Barceló (2018), whereby only the most cognitively demanding target trials immediately following a switch cue elicited additional frontal rP3 positivities, in spite of using identical visual displays as in target trials following a repeat cue. Brydges and Barceló (2018) argued that the extra cognitive demands required to categorize first target trials after a switch cue were contingent to response demands, and thus linked to the updating of low-order S–R mappings in a particular target trial. The present rP3 results are consistent with the increased response conflict in incongruent flanker trials, whereby the updating of low-level S–R mappings arguably involves concurrent selection and suppression of appropriate and inappropriate S–R links, respectively (i.e., stopping a default congruent response policy and reversing to an incongruent response policy; cf. Friston, et al. 2017). Thus, participants may adopt a default (or 'prior') congruent green-go response policy to maximize their behavioral efficiency in the most frequent and least informative congruent trials. However, when confronted with a relatively surprising incongruent green flanker stimulus, participants had to remap their low-level S–R links as part of the ongoing high-order hidden unit, which results in a frontal rP3 followed by a delayed parietal rP3 in incongruent trials indexing the S–R remapping. Relatedly, Verleger et al. (2016) found that rP3 amplitude occurring at parietal sites approximately 40 ms pre-response was positively associated with task difficulty, and also that the most cognitively demanding trials (a rare response in a two-choice task) resulted in an additional fronto-central positivity occurring approximately 90 ms pre-response, thus generally consistent with the rP3 positivities observed in the current study.

It should briefly be acknowledged that RIDE is a relatively novel technique for obtaining independent P3 subcomponents in comparison to established principal components analysis (PCA) techniques (e.g., Dien et al. 2004; Rushby et al. 2005; Spencer et al. 1999). The main

advantage of the new RIDE technique compared to conventional PCA methods is that it offers a novel and theory-guided decomposition of the P3 and LPC into stimulus-, response-locked and latency-variable P3-like subcomponents (Ouyang et al. 2017). Thus, the rationale for using RIDE rather than PCA was to revise the context updating hypothesis of P3 elicitation in the light of the new active Bayesian inference framework together with new evidence suggesting that 'the context' to be updated consists of not only the sensory units of stimulation, but also associated motor units, and intermediate high-order hidden units, all of which may need to be dynamically updated on a trial by trial basis (cf., Brydges and Barceló 2018; Friston et al. 2017; Parr et al. 2020). Indeed, the results show functionally distinct P3-like subcomponents in all the S-, R- and C-clusters, and thus offer a novel interpretative framework for the conventional context updating hypothesis of P3 elicitation in line with modern views from the Bayesian brain hypothesis.

Limitations

The current study did have some limitations. First, it should be acknowledged that there is a degree of subjectivity in the selection of latency windows for the S-, C-, and R-clusters, which can potentially affect results. In the current study, the latency windows of the S- and C-clusters did not greatly overlap, which limits the likelihood of a latency-variable N2 component to be observed (although a small stimulus-locked parietal positivity modulation was observed). Previous research that decomposed the N2 component has been mixed with regards to observing an N2 component in the C-cluster (e.g., Chmielewski et al. 2018; Ouyang et al. 2013). Additionally, some observed peaks were not picked up well by the selected time windows (e.g., the sN2 peak at Pz). This is likely to be partly due to the time windows being chosen based on previous research and the ERP data (following the guidelines outlined by Keil et al. 2014), after which the RIDE decomposition procedure adjusted the latency of the peaks within each trial. Given problems with and recommendations to avoid using flexibility in data analysis (e.g., Carp 2012a, b; Luck and Gaspelin 2017; Poldrack et al. 2017; Simmons et al. 2011), it was agreed that adjusting these time windows would misrepresent the study and could affect the replicability of the findings. Regardless, future researchers could employ more data-driven approaches to identification of time windows, and/or preregister their analysis plan prior to data collection (Nosek et al. 2018).

Conclusions

The current study examined whether one, two, or three high-order hidden units could account for the pattern of frontal N2 and P3 potentials in go/nogo version of a flanker task. This question was examined under the light of novel findings that conventional N2 and P3 ERP components can be decomposed into stimulus-locked, latency variable, and response-locked component processes. Overall, the results from the RIDE analyses are consistent with previous findings about a multiplicity of functionally distinct target P3-like subcomponents (Barcelo and Cooper 2018a, b; Brydges and Barceló 2018), and are an extension of (yet consistent with) seminal early research investigating potential distinctions between the P3a, P3b, and LPC components (e.g., Courchesne et al. 1975; Dien et al. 2004; Donchin and Coles 1988; Johnson and Donchin 1985; Pritchard 1981; Snyder and Hillyard 1976; Spencer et al. 1999; Squires et al. 1975). Altogether, our RIDE results offer a highly dynamic picture whereby one, two, and at least three high-order hidden frontal units were inferred to be engaged at different time windows (as indexed by different ERP/RIDE subcomponents) to account for performance on the flanker task. These positivities overlay fronto-parietal scalp regions, with the amount of frontal recruitment depending on dynamic split-second changes in transmitted information (i.e., cognitive load; Miller 1956; Fan 2014; Zénon et al. 2019), supporting Koechlin and Summerfield's (2007) rostro-caudal axis of cognitive control and Miller and Cohen's (2001) integrative theory of prefrontal function. In conclusion, this study provides the first evidence that behavioral congruency effects relate to delayed neural information processing indexed by response-locked P3-like potentials overlying fronto-parietal regions (cf., R-cluster; Figs. 6, 7). Further, these delays in response-locked neural activity resulted from the accumulative effect of earlier and distinct RIDE congruency effects starting in the S- and C-clusters (that is, involving both stimulus-locked and non-phase locked neural activity overlying frontal and parietal regions). Finally, these findings show that successful conflict detection and context updating are associated with a distinct combination of stimulus-locked, response-locked and latency variably electrophysiological processes putatively reflecting split-second neural dynamics across a cingulo-fronto-parietal network for cognitive control (Botvinick et al. 2004; Duncan 2010; Fan 2014; Niendam et al. 2012).

Acknowledgements The research was funded by the School of Psychological Science at the University of Western Australia. Funding support was provided for by an Australian Postgraduate Award scholarship for Christopher Brydges. The funders had no role in study design, data collection and analysis, decision to publish, or

preparation of the manuscript. The authors have declared that no competing interests exist.

References

Armitage P, McPherson CK, Rowe BC (1969) Repeated significance tests on accumulating data. J R Stat Soc Ser A (Gen) 132(2):235–244. https://doi.org/10.2307/2343787

Attneave F (1959) Applications of information theory to psychology: a summary of basic concepts, methods, and results. Holt, Oxford

Barceló F, Cooper P (2018a) An information theory account of late frontoparietal ERP positivities in cognitive control. Psychophysiology 55(3):e12814. https://doi.org/10.1111/psyp.12814

Barceló F, Cooper PS (2018b) Quantifying contextual information for cognitive control. Front Psychol 9:1693. https://doi.org/10.3389/fpsyg.2018.01693

Barceló F, Knight RT (2007) An information-theoretical approach to contextual processing in the human brain: evidence from prefrontal lesions. Cereb Cortex 17(1):i51–i60. https://doi.org/10.1093/cercor/bhm111

Bekker EM, Kenemans JL, Verbaten MN (2005) Source analysis of the N2 in a cued Go/NoGo task. Cogn Brain Res 22(2):221–231. https://doi.org/10.1016/j.cogbrainres.2004.08.011

Bell AJ, Sejnowski TJ (1995) An information-maximization approach to blind separation and blind deconvolution. Neural Comput 7(6):1129–1159. https://doi.org/10.1162/neco.1995.7.6.1129

Bledowski C, Prvulovic D, Hoechstetter K, Scherg M, Wibral M, Goebel R, Linden DE (2004) Localizing P300 generators in visual target and distractor processing: a combined event-related potential and functional magnetic resonance imaging study. J Neurosci 24(42):9353–9360. https://doi.org/10.1523/JNEUROSCI.1897-04.2004

Botvinick MM, Braver TS, Barch DM, Carter CS, Cohen JD (2001) Conflict monitoring and cognitive control. Psychol Rev 108(3):624–652. https://doi.org/10.1037/0033-295X.108.3.624

Botvinick MM, Cohen JD, Carter CS (2004) Conflict monitoring and anterior cingulate cortex: an update. Trends Cogn Sci 8(12):539–546. https://doi.org/10.1016/j.tics.2004.10.003

Brydges CR, Barceló F (2018) Functional dissociation of latency-variable, stimulus- and response-locked target P3 sub-components in task switching. Front Hum Neurosci 12:60. https://doi.org/10.3389/fnhum.2018.00060

Brydges CR, Gaeta L (2019) An introduction to calculating Bayes factors in JASP for speech, language, and hearing research. J Speech Language Hear Res 62(12):4523–4533. https://doi.org/10.1044/2019_JSLHR-H-19-0183

Brydges CR, Clunies-Ross K, Clohessy M, Lo ZL, Nguyen A, Rousset C, Fox AM (2012) Dissociable components of cognitive control: an event-related potential (ERP) study of response inhibition and interference suppression. PLoS ONE 7(3):e34482. https://doi.org/10.1371/journal.pone.0034482

Brydges CR, Anderson M, Reid CL, Fox AM (2013) Maturation of cognitive control: delineating response inhibition and interference suppression. PLoS ONE 8(7):e69826. https://doi.org/10.1371/journal.pone.0069826

Brydges CR, Fox AM, Reid CL, Anderson M (2014) Predictive validity of the N2 and P3 ERP components to executive functioning in children: a latent-variable analysis. Front Hum Neurosci 8:80. https://doi.org/10.3389/fnhum.2014.00080

Button KS, Ioannidis JP, Mokrysz C, Nosek BA, Flint J, Robinson ES, Munafò MR (2013) Power failure: why small sample size undermines the reliability of neuroscience. Nat Rev Neurosci 14(5):365–376. https://doi.org/10.1038/nrn3475

Carp J (2012a) On the plurality of (methodological) worlds: estimating the analytic flexibility of fMRI experiments. Front Neurosci 6:149. https://doi.org/10.3389/fnins.2012.00149

Carp J (2012b) The secret lives of experiments: methods reporting in the fMRI literature. NeuroImage 63:289–300. https://doi.org/10.1016/j.neuroimage.2012.07.004

Carter CS, Van Veen V (2007) Anterior cingulate cortex and conflict detection: an update of theory and data. Cogn Affective Behav Neurosci 7(4):367–379. https://doi.org/10.3758/CABN.7.4.367

Chmielewski WX, Mückschel M, Beste C (2018) Response selection codes in neurophysiological data predict conjoint effects of controlled and automatic processes during response inhibition. Hum Brain Mapp 39:1839–1849. https://doi.org/10.1002/hbm.23974

Cohen J (1994) The earth is round ($p < 0.5$). Am Psychol 49(12):997–1003. https://doi.org/10.1037/0003-066X.49.12.997

Cooper PS, Darriba Á, Karayanidis F, Barceló F (2016) Contextually sensitive power changes across multiple frequency bands underpin cognitive control. NeuroImage 132:499–511. https://doi.org/10.1016/j.neuroimage.2016.03.010

Courchesne E, Hillyard SA, Galambos R (1975) Stimulus novelty, task relevance and the visual evoked potential in man. Electroencephalogr Clin Neurophysiol 39:131–143. https://doi.org/10.1016/0013-4694(75)90003-6

Delorme A, Makeig S (2004) EEGLAB: an open source toolbox for analysis of single-trial EEG dynamics including independent component analysis. J Neurosci Methods 134(1):9–21. https://doi.org/10.1016/j.jneumeth.2003.10.009

Dien J, Spencer KM, Donchin E (2004) Parsing the "Late Positive Complex": mental chronometry and the ERP components that inhabit the neighborhood of the P300. Psychophysiology 41:665–678. https://doi.org/10.1111/j.1469-8986.2004.00193.x

Dienes Z (2011) Bayesian versus orthodox statistics: Which side are you on? Perspect Psychol Sci 6(3):274–290. https://doi.org/10.1177/1745691611406920

Donchin E (1981) Surprise!… surprise? Psychophysiology 18:493–513. https://doi.org/10.1111/j.1469-8986.1981.tb01815.x

Donchin E, Coles MG (1988) Is the P300 component a manifestation of context updating. Behav Brain Sci 11:357–427. https://doi.org/10.1017/S0140525X00058027

Doya K, Ishii K (2007) A probability primer. In: Doya K, Ishii S, Pouget A, Rao RPN (eds) Bayesian brain: probabilistic approaches to neural coding. The MIT Press, Cambridge, pp 3–13

Duncan J (2010) The multiple-demand (MD) system of the primate brain: mental programs for intelligent behaviour. Trends Cogn Sci 14(4):172–179. https://doi.org/10.1016/j.tics.2010.01.004

Duncan-Johnson CC, Donchin E (1977) On quantifying surprise: the variation of event-related potentials with subjective probability. Psychophysiology 14:456–467. https://doi.org/10.1111/j.1469-8986.1977.tb01312.x

Enriquez-Geppert S, Barceló F (2018) Multisubject decomposition of event-related positivities in cognitive control: tackling age-related changes in reactive control. Brain Topogr 31(1):17–34. https://doi.org/10.1007/s10548-016-0512-4

Falkenstein M, Hohnsbein J, Hoormann J (1994) Effects of choice complexity on different subcomponents of the late positive complex of the event-related potential. Electroencephalogr Clin Neurophysiol 92(2):148–160. https://doi.org/10.1016/0168-5597(94)90055-8

Falkenstein M, Hoormann J, Hohnsbein J (1999) ERP components in Go/Nogo tasks and their relation to inhibition. Acta Physiol (Oxf) 101(2):267–291. https://doi.org/10.1016/S0001-6918(99)00008-6

Fan J (2014) An information theory account of cognitive control. Front Hum Neurosci 8:680. https://doi.org/10.3389/fnhum.2014.00680

Farwell LA (2012) Brain fingerprinting: a comprehensive tutorial review of detection of concealed information with event-related brain potentials. Cogn Neurodyn 6(2):115–154. https://doi.org/10.1007/s11571-012-9192-2

Folstein JR, Van Petten C (2008) Influence of cognitive control and mismatch on the N2 component of the ERP: a review. Psychophysiology 45(1):152–170. https://doi.org/10.1111/j.1469-8986.2007.00602.x

Friedman D, Cycowicz YM, Gaeta H (2001) The novelty P3: an event-related brain potential (ERP) sign of the brain's evaluation of novelty. Neurosci Biobehav Rev 25(4):355–373. https://doi.org/10.1016/S0149-7634(01)00019-7

Friston K, FitzGerald T, Rigoli F, Schwartenbeck P, Pezzulo G (2017) Active inference: a process theory. Neural Comput 29(1):1–49. https://doi.org/10.1162/NECO_a_00912

Gajewski PD, Falkenstein M (2013) Effects of task complexity on ERP components in Go/Nogo tasks. Int J Psychophysiol 87(3):273–278. https://doi.org/10.1016/j.ijpsycho.2012.08.007

Gajewski PD, Stoerig P, Falkenstein M (2008) ERP-Correlates of response selection in a response conflict paradigm. Brain Res 1189:127–134. https://doi.org/10.1016/j.brainres.2007.10.076

Gratton G, Cooper P, Fabiani M, Carter CS, Karayanidis F (2018) Dynamics of cognitive control: theoretical bases, paradigms, and a view for the future. Psychophysiology 55:e13016. https://doi.org/10.1111/psyp.13016

Güntekin B, Başar E (2010) A new interpretation of P300 responses upon analysis of coherences. Cogn Neurodyn 4(2):107–118. https://doi.org/10.1007/s11571-010-9106-0

JASP Team (2018) JASP (Version 0.8.5.1) [Computer software]. https://jasp-stats.org

Jeffreys H (1961) Theory of probability. Oxford University Press, London

Jepma M, Murphy P, Nassar MR, Rangel-Gomez M, Meeter M, Nieuwenhuis S (2016) Catecholaminergic regulation of learning rate in a dynamic environment. PLoS Comput Biol 12(10):e1005171. https://doi.org/10.1371/journal.pcbi.1005171

Johnson R Jr, Donchin E (1985) Second thoughts: multiple P300s elicited by a single stimulus. Psychophysiology 22(2):182–194. https://doi.org/10.1111/j.1469-8986.1985.tb01584.x

Kałamała P, Szewczyk J, Senderecka M, Wodniecka Z (2018) Flanker task with equiprobable congruent and incongruent conditions does not elicit the conflict N2. Psychophysiology 55(2):e12980. https://doi.org/10.1111/psyp.12980

Keil A, Debener S, Gratton G, Junghöfer M, Kappenman ES, Luck SJ, Yee CM (2014) Committee report: publication guidelines and recommendations for studies using electroencephalography and magnetoencephalography. Psychophysiology 51:1–21. https://doi.org/10.1111/psyp.12147

Keysers C, Gazzola V, Wagenmakers E-J (2020) Using Bayes factor hypothesis testing in neuroscience to establish evidence of absence. Nat Neurosci 23:788–799. https://doi.org/10.1038/s41593-020-0660-4

Kieffaber PD, Hetrick WP (2005) Event-related potential correlates of task switching and switch costs. Psychophysiology 42:56–71. https://doi.org/10.1111/j.1469-8986.2005.00262.x

Koechlin E, Summerfield C (2007) An information theoretical approach to prefrontal executive function. Trends Cogn Sci 11(6):229–235. https://doi.org/10.1016/j.tics.2007.04.005

Kopp B, Lange F (2013) Electrophysiological indicators of surprise and entropy in dynamic task-switching environments. Front Hum Neurosci 7:300. https://doi.org/10.3389/fnhum.2013.00300

Kopp B, Seer C, Lange F, Kluytmans A, Kolossa A, Fingscheidt T, Hoijtink H (2016) P300 amplitude variations, prior probabilities, and likelihoods: a Bayesian ERP study. Cogn Affective Behav Neurosci 16(5):911–928. https://doi.org/10.3758/s13415-016-0442-3

Kruschke JK (2013) Bayesian estimation supersedes the t test. J Exp Psychol Gen 142(2):573–603. https://doi.org/10.1037/a0029146

Lopez-Calderon J, Luck SJ (2014) ERPLAB: an open-source toolbox for the analysis of event-related potentials. Front Hum Neurosci 8:213. https://doi.org/10.3389/fnhum.2014.00213

Luck SJ (2014) An introduction to the event-related potential technique, 2nd edn. MIT press, Chicago

Luck SJ, Gaspelin N (2017) How to get statistically significant effects in any ERP experiment (and why you shouldn't). Psychophysiology 54:146–157. https://doi.org/10.1111/psyp.12639

Masson ME (2011) A tutorial on a practical Bayesian alternative to null-hypothesis significance testing. Behav Res Methods 43:679–690. https://doi.org/10.3758/s13428-010-0049-5

Meijer EH, Ben-Shakhar G, Verschuere B, Donchin E (2013) A comment on Farwell (2012): brain fingerprinting: a comprehensive tutorial review of detection of concealed information with event-related brain potentials. Cogn Neurodyn 7(2):155–158. https://doi.org/10.1007/s11571-012-9217-x

Miller GA (1956) The magical number seven, plus or minus two: some limits on our capacity for processing information. Psychol Rev 63(2):81–97. https://doi.org/10.1037/0033-295X.101.2.343

Miller EK, Cohen JD (2001) An integrative theory of prefrontal cortex function. Annu Rev Neurosci 24(1):167–202. https://doi.org/10.1146/annurev.neuro.24.1.167

Mognon A, Jovicich J, Bruzzone L, Buiatti M (2011) ADJUST: an automatic EEG artifact detector based on the joint use of spatial and temporal features. Psychophysiology 48(2):229–240. https://doi.org/10.1111/j.1469-8986.2010.01061.x

Nguyen AT, Moyle JJ, Fox AM (2016) N2 and P3 modulation during partial inhibition in a modified go/nogo task. Int J Psychophysiol 107:63–71. https://doi.org/10.1016/j.ijpsycho.2016.07.002

Niendam TA, Laird AR, Ray KL, Dean YM, Glahn DC, Carter CS (2012) Meta-analytic evidence for a superordinate cognitive control network subserving diverse executive functions. Cogn Affective Behav Neurosci 12(2):241–268. https://doi.org/10.3758/s13415-011-0083-5

Nieuwenhuis S, Yeung N, Cohen JD (2004) Stimulus modality, perceptual overlap, and the go/no-go N2. Psychophysiology 41(1):157–160. https://doi.org/10.1046/j.1469-8986.2003.00128.x

Nosek BA, Ebersole CR, DeHaven AC, Mellor DT (2018) The preregistration revolution. Proc Natl Acad Sci 115(11):2600–2606. https://doi.org/10.1073/pnas.1708274114

Ouyang G, Herzmann G, Zhou C, Sommer W (2011) Residue iteration decomposition (RIDE): a new method to separate ERP components on the basis of latency variability in single trials. Psychophysiology 48:1631–1647. https://doi.org/10.1111/j.1469-8986.2011.01269.x

Ouyang G, Schacht A, Zhou C, Sommer W (2013) Overcoming limitations of the ERP method with residue iteration decomposition (RIDE): a demonstration in go/no-go experiments. Psychophysiology 50(3):253–265. https://doi.org/10.1111/psyp.12004

Ouyang G, Sommer W, Zhou C (2015) A toolbox for residue iteration decomposition (RIDE)-A method for the decomposition, reconstruction, and single trial analysis of event related potentials. J Neurosci Methods 250:7–21. https://doi.org/10.1016/j.jneumeth.2014.10.009

Ouyang G, Sommer W, Zhou C (2016) Reconstructing ERP amplitude effects after compensating for trial-to-trial latency jitter: a solution based on a novel application of residue iteration decomposition. Int J Psychophysiol 109:9–20. https://doi.org/10.1016/j.ijpsycho.2016.09.015

Ouyang G, Hildebrandt A, Sommer W, Zhou C (2017) Exploiting the intra-subject latency variability from single-trial event-related potentials in the P3 time range: a review and comparative evaluation of methods. Neurosci Biobehav Rev 75:1–21. https://doi.org/10.1016/j.neubiorev.2017.01.023

Parr T, Rikhye RV, Halassa MM, Friston KJ (2020) Prefrontal computation as active inference. Cereb Cortex 30(2):682–695. https://doi.org/10.1093/cercor/bhz118

Poldrack RA, Baker CI, Durnez J, Gorgolewski KJ, Matthews PM, Munafò MR, Yarkoni T (2017) Scanning the horizon: towards transparent and reproducible neuroimaging research. Nat Rev Neurosci 18(2):115–126. https://doi.org/10.1038/nrn.2016.167

Polich J (2007) Updating P300: an integrative theory of P3a and P3b. Clin Neurophysiol 118(10):2128–2148. https://doi.org/10.1016/j.clinph.2007.04.019

Pritchard WS (1981) Psychophysiology of P300. Psychol Bull 89:506–540. https://doi.org/10.1037/0033-2909.89.3.506

Raferty AE (1995) Bayesian model selection in social research. Sociol Methodol 25:111–164. https://doi.org/10.2307/271063

Ranganath C, Rainer G (2003) Cognitive neuroscience: neural mechanisms for detecting and remembering novel events. Nat Rev Neurosci 4(3):193–202. https://doi.org/10.1038/nrn1052

Ruchkin DS, Sutton S (1983) Positive slow wave and P300: association and dissociation. In: Gaillard AWK, Ritter W (eds) Tutorials in ERP research: endogenous components. North-Holland Publishing Company, Amsterdam, pp 233–250

Rushby JA, Barry RJ, Doherty RJ (2005) Separation of the components of the late positive complex in an ERP dishabituation paradigm. Clin Neurophysiol 116:2363–2380. https://doi.org/10.1016/j.clinph.2005.06.008

Simmons JP, Nelson LD, Simonsohn U (2011) False-positive psychology: undisclosed flexibility in data collection and analysis allows presenting anything as significant. Psychol Sci 22(11):1359–1366. https://doi.org/10.1177/0956797611417632

Simons RF, Graham FK, Miles MA, Chen X (2001) On the relationship of P3a and the Novelty-P3. Biol Psychol 56:207–218. https://doi.org/10.1016/s0301-0511(01)00078-3

Snyder E, Hillyard SA (1976) Long-latency evoked potentials to irrelevant, deviant stimuli. Behav Biol 16:319–331. https://doi.org/10.1016/S0091-6773(76)91447-4

Spencer KM, Dien J, Donchin E (1999) A componential analysis of the ERP elicited by novel events using a dense electrode array. Psychophysiology 36:409–414. https://doi.org/10.1017/s0048577299981180

Squires NK, Squires KC, Hillyard SA (1975) Two varieties of long-latency positive waves evoked by unpredictable auditory stimuli in man. Electroencephalogr Clin Neurophysiol 38:387–401. https://doi.org/10.1016/0013-4694(75)90263-1

Van Veen V, Carter CS (2002) The anterior cingulate as a conflict monitor: fMRI and ERP studies. Physiol Behav 77(4–5):477–482. https://doi.org/10.1016/S0031-9384(02)00930-7

Verleger R (1997) On the utility of P3 latency as an index of mental chronometry. Psychophysiology 34(2):131–156. https://doi.org/10.1111/j.1469-8986.1997.tb02125.x

Verleger R, Metzner MF, Ouyang G, Śmigasiewicz K, Zhou C (2014) Testing the stimulus-to-response bridging function of the oddball-P3 by delayed response signals and residue iteration decomposition (RIDE). NeuroImage 100:271–280. https://doi.org/10.1016/j.neuroimage.2014.06.036

Verleger R, Grauhan N, Śmigasiewicz K (2016) Is P3 a strategic or tactical component? Relationships of P3 sub-components to response times in oddball tasks with go, no-go and choice responses. NeuroImage 143:223–234. https://doi.org/10.1016/j.neuroimage.2016.08.049

Wagenmakers EJ (2007) A practical solution to the pervasive problems of *p* values. Psychon Bull Rev 14(5):779–804. https://doi.org/10.3758/BF03194105

Wagenmakers EJ, Marsman M, Jamil T, Ly A, Verhagen J, Love J, Morey RD (2018) Bayesian inference for psychology. Part I: theoretical advantages and potential ramifications. Psychon Bull Rev 25(1):35–57. https://doi.org/10.3758/s13423-017-1343-3

Woody CD (1967) Characterization of an adaptive filter for the analysis of variable latency neuroelectric signals. Med Biol Eng 5(6):539–554. https://doi.org/10.1007/BF02474247

Xie L, Ren M, Cao B, Li F (2017) Distinct brain responses to different inhibitions: evidence from a modified flanker task. Sci Rep 7(1):6657. https://doi.org/10.1038/s41598-017-04907-y

Yeung N, Nieuwenhuis S (2009) Dissociating response conflict and error likelihood in anterior cingulate cortex. J Neurosci 29(46):14506–14510. https://doi.org/10.1523/JNEUROSCI.3615-09.2009

Zénon A, Solopchuk O, Pezzulo G (2019) An information theoretic perspective on the costs of cognition. Neuropsychologia 123:5–18. https://doi.org/10.1016/j.neuropsychologia.2018.09.013

Zhou S, Xiong S, Cheng W, Wang Y (2019) Flanker paradigm contains conflict and distraction factors with distinct neural mechanisms: an ERP analysis in a 2-1 mapping task. Cogn Neurodyn 13:341–356. https://doi.org/10.1007/s11571-019-09529-w